Desalination and Water Treatment
www.deswater.com
doi: 10.1080/19443994.2014.946726

55 (2015) 3343–3349
September

Taylor & Francis
Taylor & Francis Group

Heat transfer characteristics of horizontal tube falling film evaporation for desalination

Shengqiang Shen*, Xue Chen, Xingsen Mu, Yaoxuan Wang, Luyuan Gong

School of Energy and Power Engineering, Dalian University of Technology, Dalian 116024, China, Tel. +86 411 84708464; Fax: +86 411 84707963; email: zzbshen@dlut.edu.cn (S. Shen)

Received 24 March 2014; Accepted 16 June 2014

ABSTRACT

An experimental study on heat transfer characteristics of falling film evaporation outside horizontal tube was carried out at low evaporation temperature. The Al-brass tubes with 19 mm outer diameter and 1,600 mm effective length were adopted and arranged vertically in the evaporator. The electric heater was fixed tightly in the test tube for generating uniform heat flux. And thermocouples were installed in the surface of the test tube to measure surface temperatures. The experimental fluids are water and seawater with salinity of 1.5, 3, and 4.5%. The variations of heat transfer coefficient h were studied in detail with saturation temperament ranging from 50 to 70˚C, the spray density Γ ranging between 0.017 and 0.087 $kg\,m^{-1}\,s^{-1}$, and the heat flux q varying from 7.75 to 12.30 $kW\,m^{-2}$. The results show that the average heat transfer coefficients of both water and seawater increase with the spray density until about 0.052 $kg\,m^{-1}\,s^{-1}$. The heat transfer coefficient of fresh water increases with evaporation temperature whereas that of the seawater decreases slightly with the evaporation temperature. The average heat transfer coefficient decreases with salinity. In addition, the circumferential distribution of local heat transfer coefficients and the effect of defoamer on heat transfer are studied.

Keywords: Horizontal tube falling film evaporation; Desalination; Heat transfer coefficient; Seawater

1. Introduction

Horizontal tube falling film evaporation has obvious advantages of high heat transfer coefficient and low temperature difference, compared with the vertical tube and flooded tube evaporation [1]. Furthermore, the suitability for low temperature difference heat transfer and the good performance of anti-scale also make this technology become the most effective methods for the low-temperature multi-effect distillation (LT-MED) desalination.

Due to the heat transfer coefficient of the evaporation outside tubes is about 50% of that of the condensation inside tubes, the overall heat transfer coefficient is mainly dominated by the falling film evaporation outside tubes. Many prior studies on horizontal tube falling film evaporation involving different fluids,

*Corresponding author.

Presented at the Conference on Desalination for the Environment: Clean Water and Energy 11–15 May 2014, Limassol, Cyprus

apparatuses and working conditions have been reported. A detailed review was provided by Ribatski and Jacobi [2] with the focus on the studies before 2005.

Ganic and Roppo [3] conducted an experiment with 25.4 mm diameter copper tube at the spray density ranging from about 0.007 to 0.040 kg m^{-1} s^{-1}, the results show that the average heat transfer coefficients of water increases with the tube spacing and spray density.

Parken and Fletcher [4] and Parken et al. [5] studied the heat transfer coefficient of falling film around 25.4- and 50.8-mm-diameter brass tubes, taking water as experimental fluid. Their report indicated that the average heat transfer coefficients increase with the evaporation temperature and spray density, but decrease with tube diameter. A distribution of local heat transfer coefficients along circumferential angle was presented.

Hu and Jacobi [6] did an investigation on 15.88-, 19.05-, and 22.22-mm-diameter tubes with water, glycol and glycol aqueous solution in the range of spray density from 0 to 0.36 kg m^{-1} s^{-1}. The research shows that the heat transfer coefficients increase with the spray density and tube spacing and decrease with the tube diameter. A similar distribution of local heat transfer coefficient with Parken et al. [5] was observed.

Fletcher et al. studied the falling film evaporation of water [7] and natural seawater with 3.45% salinity [8] around 25.4 and 50.8-mm diameter Ni–Cu tubes under boiling condition. The results show that the heat transfer coefficients increase with heat flux. Moreover, Fletcher et al. [8] indicated that the heat transfer coefficient of seawater is higher than that of the freshwater.

Mu et al. [9] conducted a comparative experiment between water and natural seawater with 25.4-mm Al-brass tubes, focusing the heat transfer characteristics at the evaporation temperature between 50 and 70 °C and the spray density within 0.026–0.087 kg m^{-1} s^{-1}. They pointed out that the heat transfer coefficient of natural seawater is lower than freshwater. With the evaporation temperature increase, the heat transfer coefficient of fresh water increases, whereas the coefficient of natural seawater decreases. With the spray density increases, the heat transfer coefficient increases sharply at the beginning, then the increase gradually slows down and even decreases.

However, because of the diversity of experimental facilities in different literatures and the complexity of the heat transfer process, divergences still exist in some aspects. Furthermore, in previous experimental studies, only a few studies did experiments with natural seawater to simulate the real process of horizontal tube falling film evaporation in desalination plant. Due to the complexity of natural seawater components, a large difference exists in thermophysical properties between natural seawater and fresh water. Thus, the experimental studies of falling film evaporation should be carried out further to provide data of LT-MED desalination under the same conditions.

2. Experimental apparatus

Fig. 1 shows the schematic diagram of this experiment apparatus. It contains a fluid circle and an evaporation/condensation cycle. A test vessel installed with associated instruments for measuring temperature, pressure, and flow rate is located in the junction of the two cycles. In the fluid circle, the experimental fluid is pumped from the reservoir to the upper tank and then passes through the rotameter to the feed tube in the test vessel. The fluid is partially evaporated in the vessel, and the un-evaporated fluid is pumped back to the reservoir. In the evaporation/condensation cycle, the fluid is heated by the test tube in the vessel, and the vapor evaporated from the film around the test tube is delivered to the condenser. While the experimental fluid is seawater, the condensate is returned to the reservoir in time for keeping the salinity.

Fig. 2 shows the arrangement of tubes in the test vessel. The topmost tube is a feed tube which distributes liquid on the downward tube. The second to the fourth tubes are dummy tubes which are used for forming stable falling film flow pattern. The bottom one is a heating tube as the test tube. The surface of

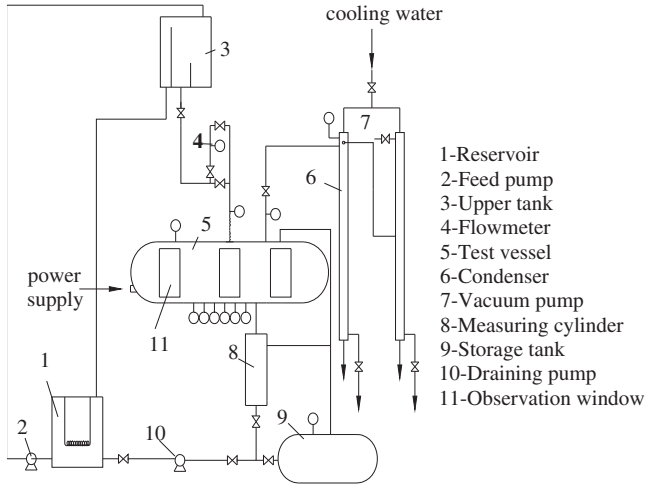

Fig. 1. Schematic diagram of the experimental apparatus.

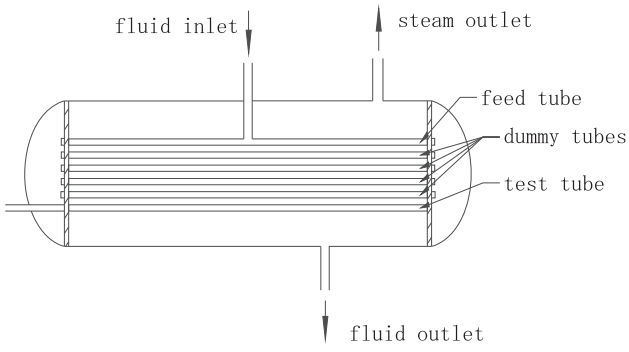

Fig. 2. Arrangement of the tubes.

the made-to-order heater core attached tightly to the internal surface of the test tube for generating uniform heat flux. All the tubes are made of Al-brass with the outer diameter of 19 mm and the effective length of 1,600 mm. The tube pitch is 34.2 mm (1.8 times the outer diameter of tube in this experiment). Eighty holes are drilled in a line on the bottom of the feed tube for distributing fluid. According to the Taylor's instability equation, the hole spacing is determined as 20 mm and hole diameter is 1.5 mm [10].

Fig. 3 shows the installation of thermocouples. Twenty thermocouples are embedded axially and welded tightly in the wall of the tube. The surface is polished carefully to eliminate the impact on fluid flow. Numerous repeated experiments under each condition were conducted for collecting enough data for assuring the accuracy and rationality.

The pressures of the test vessel are measured by pressure sensors with the measuring range from −0.1 to 0 MPa, the precision of 0.2 kPa, and the error within 0.5%. The measuring range of the rotameter is from 100 to 1,000 L h^{-1} with the error less than 1.5%. The calibration of thermocouples is done before experiment to make sure the precision is within ±0.05℃.

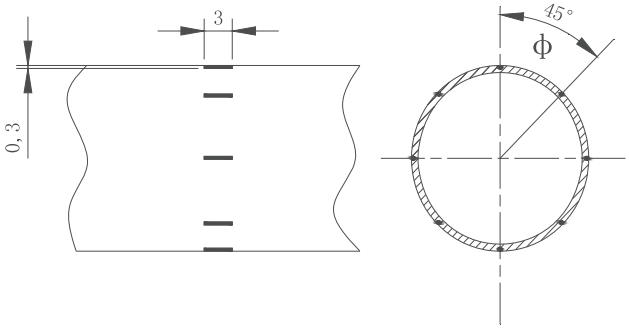

Fig. 3. Structure diagram of test tube.

In this experiment, both the water and natural seawater were used as experimental fluid. The natural seawater was collected from the Yellow Sea near Dalian in summer with 3.0% salinity. For experimental fluid with different salinities, the seawater with 4.5% salinity is concentrated from natural seawater, and the seawater with 1.5% salinity is obtained by diluting natural seawater with pure water. Because of the rich surface-active substance in natural seawater, a large number of foams will be generated and stay stable in the fluid when seawater flows. Hence, one of the polyether-modified polysiloxane is added in natural seawater with 0.1 ppm as a defoamer in the whole experimental process if not specified.

3. Experiment result and discussion

For simulating the typical operating condition in LT-MED desalination plant, the evaporation temperature is regulated from 50 to 70℃ by adjusting the negative pressure in the test vessel, and the spray density is controlled in the range from 0.017 to 0.087 kg m^{-1} s^{-1}.

The heat transfer coefficient is calculated by the formula as follow:

$$h_a = \frac{Q}{F(T_a - T_{\text{sat}})} = \frac{q}{\Delta T_a} \tag{1}$$

h_a is the average heat transfer coefficient; Q is the power, calculated by the working voltage and current of heating; F is the area of tube surface; T_{sat} is the saturation temperature; T_a is the average surface temperature; ΔT_a is the difference between the saturation temperature and the average surface temperature measured by thermocouples; q is heat flux.

Because of the different status of the film around the tube, the local heat transfer coefficients are different either. In this experiment, the data of local temperature are measured by thermocouples fixed circumferentially on the tube surface. The local heat transfer coefficient can be obtained according to the following formula:

$$h_l = \frac{q}{\Delta T_l} \tag{2}$$

in Eq. (2), h_l is the local heat transfer coefficient; ΔT_l is the difference between local wall temperature and saturation temperature.

3.1. The effect of heat flux

Fig. 4 shows the distributions of average heat transfer coefficients with three different heat fluxes at $\Gamma = 0.052\ kg\ m^{-1}\ s^{-1}$; the points in this scatter diagram are instantaneous values which are obtained in seconds. In Fig. 4, it can be easily found that the h_a of water and seawater distribute separately in a relative small range, although the heat flux varies.

Fig. 5 shows the general variation of h_a under different heat flux with seawater as experimental fluid and the spray density ranged from 0.017 to 0.087 kg $m^{-1}\ s^{-1}$ at 60℃. From Fig. 5, it also can be seen that the three profiles of h_a are almost similar, hence the heat flux hardly affects the h_a under the strict convective conditions.

3.2. The effect of spray density

The variations of heat transfer coefficient of water and seawater ($s = 3\%$) with different spray density from 50 to 70℃ are shown in Figs. 6 and 7, respectively. It can be seen that the h_a of both water and seawater present a similar tendency: the curves of h_a increase with the Γ at first, then decrease as Γ reaches about $0.052\ kg\ m^{-1}\ s^{-1}$. The augment of heat transfer coefficients becomes less obvious, and the heat transfer coefficients begin to decline slightly.

The flow velocity increases with Γ at low spray density because the enhancement of the falling film fluctuation improves the heat transfer. Although the liquid film also thickens with Γ, the fluctuation still dominates the impacts. However, when the Γ exceeds about $0.052\ kg\ m^{-1}\ s^{-1}$, the further increase in film thickness leads to a suppressing impact on the disturbance, and results in slight decrease in h_a.

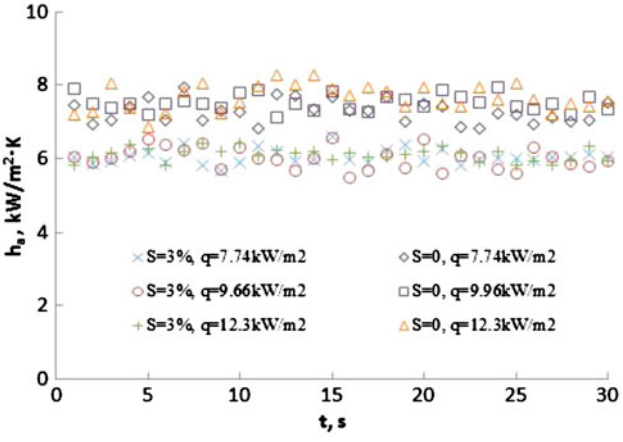

Fig. 4. The effect of heat flux vs. time at $\Gamma = 0.052\ kg\ m^{-1}s^{-1}$.

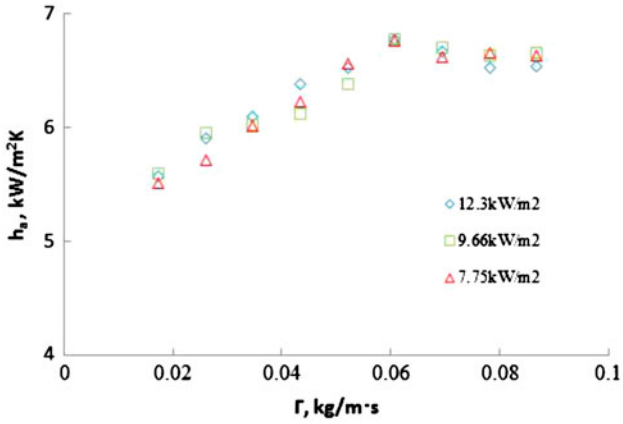

Fig. 5. The effect of heat flux vs. Γ at 60℃.

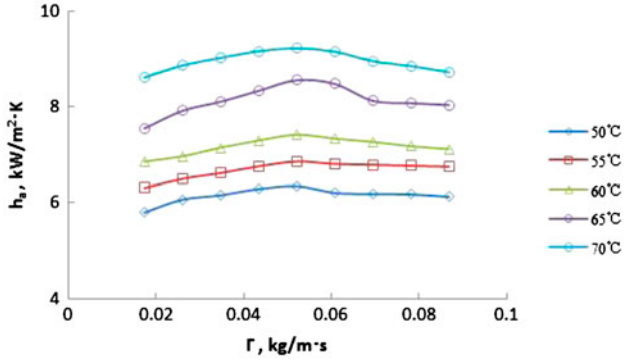

Fig. 6. The effect of Γ on h_a of water.

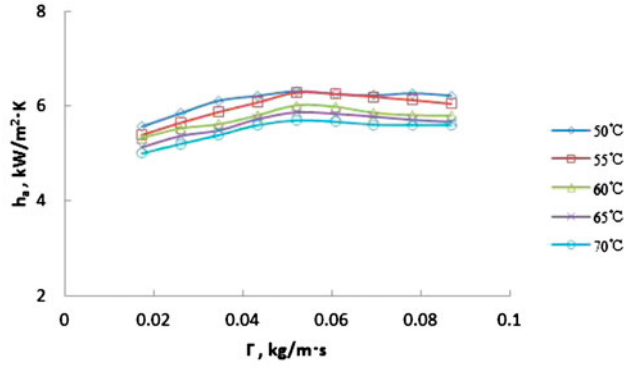

Fig. 7. The effect of Γ on h_a of seawater with 3% salinity.

3.3. The effect of evaporation temperature

Fig. 6 clearly demonstrates that the h_a of water increases with the evaporation temperature. This phenomenon may be caused by the reasons as follows. Firstly, the decline of viscosity makes the film thinner

and the velocity higher. Secondly, the decline of surface tension helps to improve heat transfer on the account of the weaker suppression of the liquid film fluctuation. Thirdly, the thermal conductivity of fresh water increases as temperature increases. All the three factors above lead to the increase of h_a with evaporation temperature.

Comparing with water, the curves of h_a of natural seawater show a different tendency. The h_a does not increase with the temperature. It even displays a downward trend with evaporation temperature. A similar tendency is observed by Mu et al. [9] with 25.4-mm diameter tube. This phenomenon illustrates that the variation of natural seawater heat transfer characteristic vs. temperature is unlike as water. It may be caused by the special physical properties of seawater or the release of carbon dioxide in the evaporation. However, due to the limitation of studies on natural seawater properties [11] and the complexity of the seawater evaporation process, a reasonable quantitative explanation for this phenomenon cannot be concluded yet.

3.4. The effect of salinity

The effect of salinity on h_a with $T_{sat} = 60$°C is shown in Fig. 8. The h_a shows an obvious decrease with salinity. This is because that both the viscosity and surface tension increase with the salinity [11]. Furthermore, for aqueous solutions containing electrolytes such as seawater, the thermal conductivity usually decreases as the increase of the dissolved salts concentration [11].

From the results of this section as well as Section 3.3, it can be seen that there are many noteworthy differences in heat transfer between the natural seawater and water. Consequently, a further study on natural seawater properties and heat transfer characteristics will be carried out subsequently for the horizontal tube falling film evaporation.

3.5. The distribution of local heat transfer coefficient

Several typical distributions of h_l around the tube circumferentially under $q = 7.75\ \mathrm{kW\ m^{-2}}$ are presented in Fig. 9. It can be seen that the highest local heat transfer coefficient is at 0°. The h_l decreases rapidly during 0°–135° and slightly increases after then. Under strict convective condition, the local heat transfer coefficient depends mainly on the flow pattern. The impingement on the top of the tube results in heat transfer enhancement. The flow becomes steadier as the Φ increases and results in h_l decline. However, the h_l increases after 135° due to the liquid film fluctuation, which is caused by the accumulation and dripping at the bottom of the tube.

From above, it can be noted that the impingement region possesses the highest h_l and influences the heat transfer in the following region persistently. Therefore, in some analytical studies of the horizontal tube falling film evaporation heat transfer, simplifying the heat transfer model by neglecting impingement region is not reasonable.

Furthermore, Fig. 9 also indicates that the local heat transfer coefficients of natural seawater are generally smaller than water, especially at the top area. Because the viscosity and surface tension of seawater are larger than that of water, the fluctuation caused by the impingement is less violent. As a result, the heat transfer is weakened.

In addition, the raise of temperature results in a decrease of viscosity and surface tension of water. This decrease makes the fluctuation in liquid film more severe and thus promotes the heat transfer. Similarly, the increase in velocity also strengthens the heat transfer.

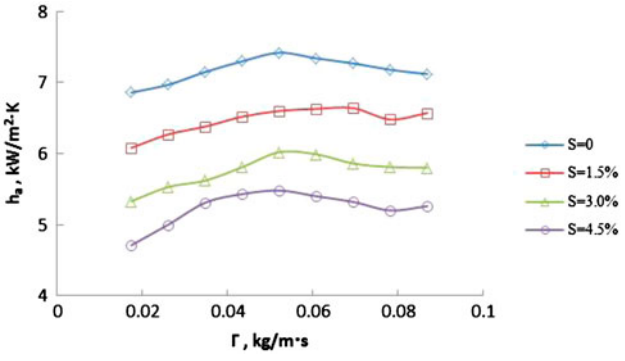

Fig. 8. The effect of salinity.

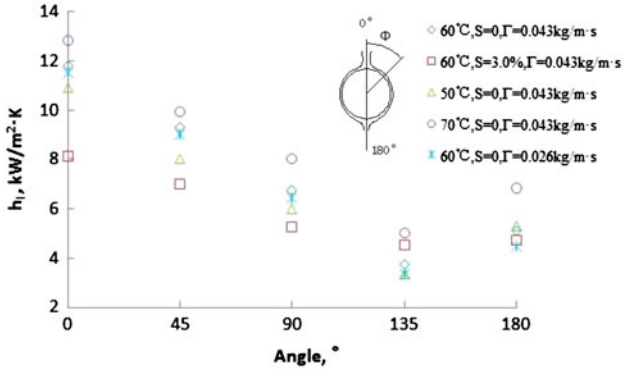

Fig. 9. The distribution of h_l.

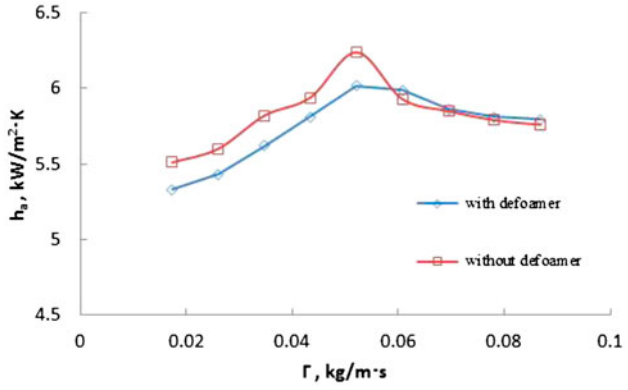

Fig. 10. The effect of defoamer on h_a at $T_{sat} = 60$ ℃.

3.6. The effect of defoamer

The polyether-modified polysiloxane is a defoamer used in desalination for its nontoxicity, stability, low addition and high efficiency. The defoamer can spread along the gas–liquid interface rapidly and reduce the surface tension to promote bubble burst and inhibit bubble formation. A preliminary exploration is conducted to investigate the effect of defoamer on the falling film evaporation heat transfer.

Fig. 10 describes the effects of the defoamer on h_a at $T_{sat} = 60$ ℃ and $s = 3\%$. This figure indicates that the h_a of seawater without defoamer is about 3% higher than the one with defoamer at Γ less than 0.052 kg m^{-1} s^{-1}. But the difference between the presence and absence of defoamer is not significant when Γ is over 0.6 kg m^{-1} s^{-1}. An understanding for this is that the generation and breakage of bubbles promote the fluctuation of liquid film and result in the improving of heat transfer. When the film becomes thicker and more fluctuant with Γ, the effect of breakage is weakened so that both curves become consistent. It could be concluded that the influence of defoamer does not make a significant impact on heat transfer.

4. Conclusion

(1) The heat transfer coefficient is almost independent of the heat flux under strict convective condition, both for the water and seawater.
(2) The average heat transfer coefficient increases with spray density at first, and then decreases slightly. For the tube with 19 mm diameter, the maximum heat transfer coefficient achieved is at Γ = 0.052 kg m^{-1} s^{-1}.
(3) The average heat transfer coefficient of water increases with evaporation temperature; whereas the average heat transfer coefficient of natural seawater shows a reverse trend with the evaporation temperature.
(4) The average heat transfer coefficient of water is larger than natural seawater under the same condition. And the average heat transfer coefficient of sea water decreases with salinity.
(5) Along the circumferential direction, the local heat transfer coefficient decreases at first and then increases slightly after about 135˚.
(6) The heat transfer coefficient of seawater with defoamer is slightly smaller than that without defoamer at low spray density. No obvious difference was observed at high spray density.

Acknowledgment

The research is supported by the Natural Science Foundation of China (No. 51176017) and Research Fund for the Doctoral Program of Higher Education of China (20110041110032).

Symbol		Description (units)
d	—	diameter (mm)
F	—	heating area (m^2)
h	—	heat transfer coefficient (kW m^{-2} ℃$^{-1}$)
h_a	—	average heat transfer coefficient (kW m^{-2} ℃$^{-1}$)
h_l	—	local heat transfer coefficient (kW m^{-2} ℃$^{-1}$)
Q	—	power (kW)
q	—	heat flux (kW m^{-2})
s	—	salinity (%)
ΔT	—	temperature difference (℃)
T_{sat}	—	saturation temperature (℃)
Γ	—	spray density per side (kg m^{-1} s^{-1})
Φ	—	the circumferential angle around the tube (˚)

References

[1] A.D. Khawaji, I.K. Kutubkhanah, Advances in seawater desalination technologies, Desalination 221(1–3) (2008) 47–69.
[2] G. Ribatski, A.M. Jacobi, Falling-film evaporation on horizontal tubes—A critical review, Int. J. Refrig. 28 (2005) 635–653.
[3] N.E. Ganic, N.M. Roppo, An experimental study of falling liquid film breakdown on a horizontal cylinder during heat transfer, J. Heat Transfer 102 (1980) 342–346.
[4] W.H. Parken, L.S. Fletcher, Heat transfer in thin liquid films flowing over horizontal tubes, Proceedings of the Seventh International Heat Transfer, Munich (1982) 415–420.

[5] W.H. Parken, L.S. Fletcher, V. Sernas, J.C. Han, Heat transfer through falling film evaporation and boiling on horizontal tubes, J. Heat Transfer 112 (1990) 744–750.
[6] X. Hu, A.M. Jacobi, The intertube falling film: Part 2—Mode effects on sensible heat transfer to a falling liquid film, J. Heat Transfer 118 (1996) 626–633.
[7] L.S. Fletcher, V. Sernas, L. Galowin, Evaporation from thin water films on horizontal tubes, Ind. Eng. Chem. Process Des. Dev. 13 (1974) 265–269.
[8] L.S. Fletcher, V. Sernas, W.H. Parken, Evaporation heat transfer coefficients for thin sea water films on horizontal tubes, Ind. Eng. Chem. Process Des. Dev. 14 (1975) 411–416.
[9] X.S. Mu, S.Q. Shen, Y. Yang, X.H. Liu, Experimental study of falling film evaporation heat transfer coefficient on horizontal tube, Desalin. Water Treat. 50 (2012) 310–316.
[10] D. Yung, J.J. Lorenz, E.N. Ganić, Vapor/liquid interaction and entrainment in falling film evaporators, J. Heat Transfer 102(1) (1980) 20–25.
[11] M.H. Sharqawy, J.H. Lienhard, S.M. Zubair, Thermophysical properties of seawater: A review of existing correlations and data, Desalin. Water Treat. 16(1–3) (2010) 354–380.